On the feasibility of DVB-T based passive radar with a single receiver channel

***Osama Mahfoudia*[*,†]*, François Horlin*[†]*, Xavier Neyt*[*]

[*]*CISS Department, Royal Military Academy, Brussels, Belgium*
[†]*OPERA Department, Université Libre de Bruxelles, Brussels, Belgium*

Keywords: Passive radar, DVB-T, reference signal reconstruction, static clutter rejection, single receiver.

Abstract

The DVB-T signals are an attractive illumination source for the passive radars due to their wide bandwidth and signal structure. The DVB-T standard permits the reconstruction of the received signal to enhance its signal-to-noise ratio (SNR). The signal reconstruction possibility allows the use of a simplified configuration of the radar by employing a single receiver. In this paper, we propose an optimized processing scheme for the single receiver DVB-T passive radar. We carry out Monte-Carlo simulations to assess the performances of the single receiver configuration, and we present real-data results to validate the proposed scheme.

1 Introduction

Passive radars employ signals from non-cooperative transmitters for target detection and tracking. Their major advantages are low cost, intercept immunity and ease of deployment. Telecommunication and broadcasting signals can be exploited as illuminators of opportunity for passive radars [1–3].

DVB-T signals as an illumination source for the passive radars have been the subject of a growing interest [4]. This is due to the suitable characteristics of the DVB-T waveform (wide bandwidth and data-independent spectrum), the high radiated power of the transmitter, and the possibility of recovering the transmitted signal [4–7].

The classical passive radar architecture involves two receiving channels. A reference channel for the reception of the direct-path signal and a surveillance channel for the reception of the target return signal. In addition to the target return, the surveillance channel collects reflections from the static scatterers (static clutter), and a direct-path signal. The direct-path signal is the most significant part of the surveillance signal which may mask the target return and reduces the detection dynamic range.

The DVB-T standard allows the reconstruction of the received reference signal to enhance its signal-to-noise ratio (SNR) [4–7]. Therefore, one can exploit the direct-path signal present in the surveillance signal to estimate a synthetic reference signal. A specific channel to acquire the reference signal is thus unnecessary which reduces the complexity and the cost of the system.

The single receiver DVB-T based passive radar approach has been initiated in [8, 9]. In this paper, we consider a single receiver DVB-T passive radar and we propose an optimized processing scheme. We employ Monte-Carlo simulations to assess the performance of the single receiver configuration and we present real-data results.

This paper is organized as follows. Section 2 presents the signal model and the signal processing scheme. Section 3 evaluates the impact of the direct-path signal power level on the detection probability. Section 4 shows the real-data results. And Section 5 concludes the paper.

2 Signal processing

2.1 Signal model

Figure 1 illustrates the configuration of a single receiver passive radar. The received signal includes the direct-path signal, the static clutter resulting from the static scatterers in the surveillance area, the thermal noise, and a possible target return. We adopt the following model for the received signal

$$x(n) = \sum_{l=0}^{L-1} h_l s(n-l) + \alpha s(n-\tau) e^{j2\pi f_d n} + v(n) \quad (1)$$

we consider L static scatterers with reflection coefficients h_l (assumed to be invariant over the processing time). The thermal noise $v(n)$ has a zero mean and a variance of σ_v^2. The target return is a time-delayed (τ), frequency-shifted (f_d), and attenuated (with a coefficient α) copy of the transmitted signal $s(n)$. We define the direct-path-to-noise ratio (DNR) as

$$\text{DNR} = |h_0|^2 \sigma_s^2 / \sigma_v^2, \quad (2)$$

where σ_s^2 is the transmitted signal variance. The target signal-to-noise ratio (SNR) is defined as follows

$$\text{SNR} = |\alpha|^2 \sigma_s^2 / \sigma_v^2. \quad (3)$$

The DVB-T standard employs the orthogonal frequency division multiplexing (OFDM) modulation scheme. One DVB-T

symbol is formed by K orthogonal subcarriers as follows

$$s(n) = \sum_{k=0}^{K-1} C_k e^{j2\pi f_k n}, \tag{4}$$

where f_k is the frequency of the k^{th} subcarrier and C_k is the k^{th} quadrature amplitude modulation (QAM) symbol. Among the K subcarriers, there are pilot subcarriers which are employed for signal synchronization and propagation channel estimation.

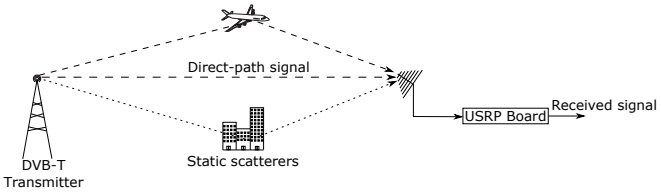

Fig. 1: DVB-T based passive radar with a single receiver.

2.2 Signal synchronization

The received signal synchronization includes the time and carrier frequency offset (CFO) estimation and compensation. The carrier frequency offset emerges from the frequency mismatch between the receiver local oscillator and the signal carrier. The pre-FFT synchronization exploits the guard interval correlation to estimate the coarse time and the carrier frequency offset [10]. The coarse time offset estimation identifies the beginning of the DVB-T symbol which allows a perfect placement of the FFT window, and the compensation of the CFO maintains the subcarrier orthogonality. The residual CFO can be estimated through the phase shift of the subcarrier pilots [11].

2.3 Signal extraction

Figure 2 summarizes the method employed to extract the reference signal and the target return signal form the received signal. The direct-path signal is the dominant component of the received signal which can be exploited to estimate the transmitted signal. The transmitted signal estimate can then be employed as a reference signal for the detection.

The transmitted signal is estimated by decoding and recoding the direct-path signal. The synchronized received signal is divided into frames of DVB-T symbols. Then, the guard interval is removed and the useful part of the symbol is Fourier-transformed; for each subcarrier, the result is expressed as

$$X(k) = H(k)C_k + X_t(k) + V(k), \tag{5}$$

where $H(k)$ is the frequency domain propagation channel coefficient for the k^{th} subcarrier, C_k is the transmitted QAM symbol, $X_t(k)$ is the target return contribution and V is the Fourier-transform of the noise v.

The frequency domain propagation channel ($\mathbf{H}$) is estimated exploiting the pilot subcarriers [12]. The propagation channel estimate, $\hat{\mathbf{H}}$, is employed for the QAM symbol equalization. The detection of the equalized QAM symbols, $\hat{\mathbf{C}}$, provides an estimate of the transmitted symbols. Classically, an estimate of the transmitted signal, $\hat{s}(n)$, can be obtained by mapping the detected QAM symbols, applying an inverse Fourier-transform and inserting the guard interval [5,6]. For low DNR values, the QAM detection error is considerable which creates a mismatch between the estimated signal and the transmitted one.

An optimal reconstruction method is proposed in [7] which minimizes the mean squared error (MSE) between the transmitted signal and the estimated one. It allows an optimum reconstruction of the transmitted signal even for low DNR values. The transmitted signal is formed by optimality weighted QAM symbols $\hat{\mathbf{C}}_{\text{opt}}$. We adopt this method for the reference signal reconstruction in the present work.

The extraction of the target return signal can be achieved by applying a static clutter suppression method [13–15] on the synchronized received signal. In this work, we consider the static clutter suppression method presented in [16] which employs the estimated channel response $\hat{\mathbf{H}}$ and the detected QAM symbols to estimate the static clutter signal. The clutter-free signal for the k^{th} subcarrier is obtained as follows

$$X_{filtered}(k) = X(k) - \hat{H}(k)\hat{C}_k. \tag{6}$$

The clutter-free signal $x_{filtered}(n)$ is obtained by inverse-Fourier transforming $\mathbf{X_{filtered}}$ (the frequency domain filtered signal) and inserting the guard interval.

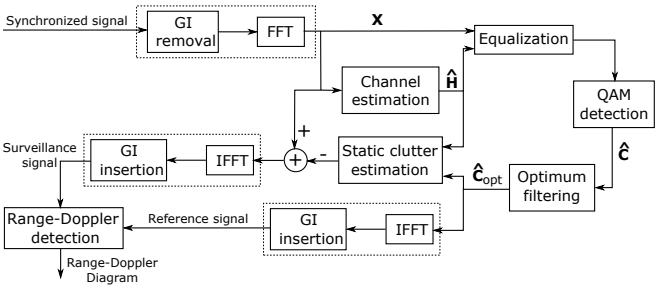

Fig. 2: Signal processing scheme.

2.4 Detection

The detection is performed by cross-correlating the filtered signal $x_{filtered}(n)$ with a time-delayed and frequency-shifted copy of the estimated transmitted signal $\hat{s}(n)$ as follows

$$\chi(\kappa, \nu) = \sum_{n=0}^{N-1} \hat{s}^*(n-\kappa) x_{filtered}(n) e^{-j2\pi\nu n}, \tag{7}$$

where κ is the time delay, ν is the frequency shift and N is the coherent integration length [4]. The result of the cross-correlation calculation is a 2D range-Doppler diagram.

3 The impact of the DNR level on the detection probability

The aim of this section is the assessment of the DNR level impact on the detection probability. Figure 3 presents Monte-Carlo simulation results for the detection probability as a function of the DNR value. The simulation was based on the processing scheme presented in the figure 2 with an integration length of $N = 10^5$, a false-alarm probability $\mathrm{P_{FA}} = 10^{-3}$, and three values of DNR.

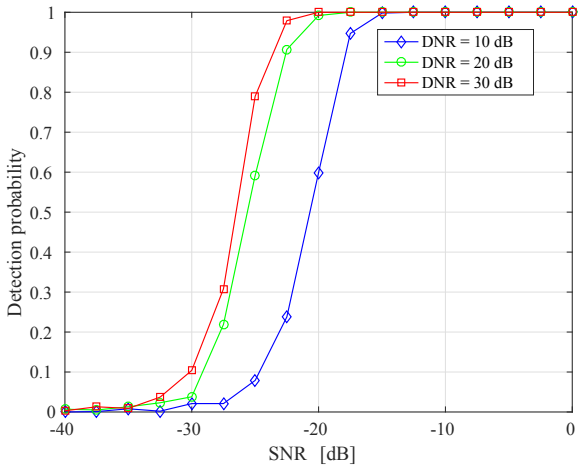

Fig. 3: Probability of detection as a function of the SNR for $N = 10^5$, $\mathrm{SNR} = -20$ dB and $\mathrm{P_{FA}} = 10^{-3}$.

The results reflect the impact of the DNR value on the detection probability. For a fixed SNR value, the detection probability for $\mathrm{DNR} = 10$ dB is lower than the one for $\mathrm{DNR} = 20$ dB and $\mathrm{DNR} = 30$ dB which is due to the QAM symbol detection error. The QAM detection error leads to a mismatch between the transmitted signal and the estimated one (which degrades the integration gain), and reduces the efficiency of the static clutter suppression.

4 Real-data results

The measurement campaign was performed in Brussels at the Royal Military Academy. We considered the DVB-T transmitter which is on the top of the Finance Tower (located at 2.5 km from the receiver) as the illuminator of opportunity. The nearby Zaventem airport (BRU) provides the opportunity of having low altitude targets during landing and taking off manoeuvres. Table 1 summarizes the measurement campaign parameters. The receiver includes a commercial Yagi antenna (dedicated for the domestic reception of DVB-T broadcasting) and a USRP B100 device. The recorded signals are stored in a host computer and processed with Matlab.

Figures 4 and 5 present the range-Doppler detection results for two data sets of 10 s duration each. For each data set, the received signal is divided into frames of 0.1 s duration. Each frame is processed as presented in figure 2. The resulting

Acquisition device	USRP B100
Sampling frequency	8 MHz
ADC resolution	12 bits
Carrier frequency	482 MHz
DVB-T mode	8k-mode
Guard interval (GI)	1/4
Transmitter radiated power	10 kW
Antenna gain	11 dBi
Transmitter-receiver distance	2.5 km
Integration time	0.1 s

Table 1: Parameters of the measurement campaign.

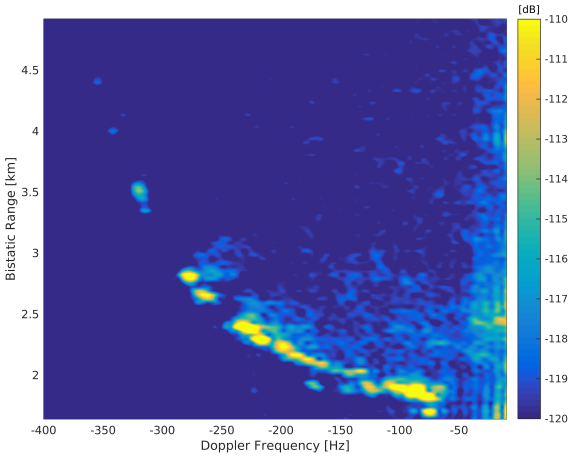

Fig. 4: Real-data results (1).

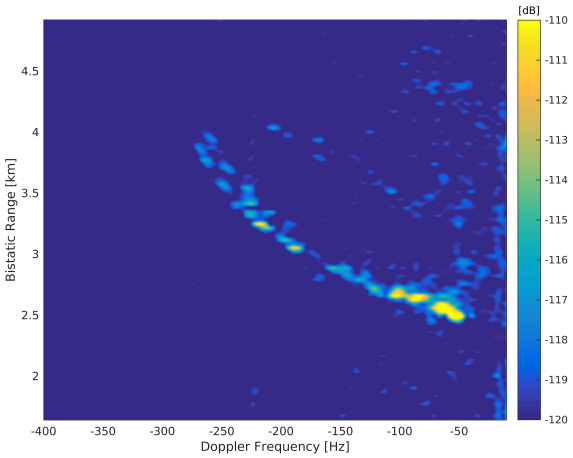

Fig. 5: Real-data results (2).

range-Doppler diagrams for the frames are summed to provide the full track of the airplane.

The results show two airplanes during the taking off manoeuvre with a bistatic range that varies between 2 km and 4 km, and a Doppler shift from 0 Hz to -350 Hz. These results validate the efficiency of the proposed processing scheme and illustrate the feasibility of a single receiver DVB-T passive radar.

5 Conclusions

The single receiver configuration is feasible thanks to the possibility of reconstructing the transmitted signal based on the received signal which includes multipath and target echoes. Employing a single receiver to build a DVB-T based passive radar reduces the system complexity and its cost. The proposed processing scheme includes an optimum signal reconstruction method and a frequency domain static clutter suppression method. The system characterization through Monte-Carlo simulation has provided an insight about the system performances for different DNR values. In the future works, we will assess the system maximum detection range.

References

[1] H. D. Griffiths and C. J. Baker, "Passive coherent location radar systems. Part 1: Performance prediction," *IEE Proceedings - Radar, Sonar and Navigation*, vol. 152, no. 3, p. 153, 2005.

[2] C. J. Baker, H. D. Griffiths, and I. Papoutsis, "Passive coherent location radar systems. Part 2: Waveform properties," *IEE Proceedings - Radar, Sonar and Navigation*, vol. 152, no. 3, p. 160, 2005.

[3] J. Palmer, S. Palumbo, A. Summers, D. Merrett, S. Searle, and S. Howard, "An overview of an illuminator of opportunity passive radar research project and its signal processing research directions," *Digital Signal Processing*, vol. 21, pp. 593–599, sep 2011.

[4] J. E. Palmer, H. A. Harms, S. J. Searle, and L. M. Davis, "DVB-T Passive Radar Signal Processing," *IEEE Transactions on Signal Processing*, vol. 61, pp. 2116–2126, apr 2013.

[5] S. Searle, S. Howard, and J. Palmer, "Remodulation of DVB-T signals for use in Passive Bistatic Radar," in *Signals, Systems and Computers (ASILOMAR), 2010 Conference Record of the Forty Fourth Asilomar Conference on*, pp. 1112–1116, nov 2010.

[6] M. Baczyk and M. Malanowski, "Reconstruction of the reference signal in DVB-T-based passive radar," *International Journal of Electronics and Telecommunications*, vol. 57, no. 1, pp. 43–48, 2011.

[7] O. Mahfoudia, F. Horlin, and X. Neyt, "Optimum reference signal reconstruction for DVB-T based passive radars," in *2017 IEEE Radar Conference (RadarConf)*, 2017.

[8] O. Mahfoudia and X. Neyt, "A DVB-T based passive radar using one USRP board," in *URSI Benelux Forum*, (Louvain-la-Neuve, Belgium), 2014.

[9] S. Searle, L. Davis, and J. Palmer, "Signal processing considerations for passive radar with a single receiver," in *2015 IEEE International Conference on Acoustics, Speech and Signal Processing (ICASSP)*, pp. 5560–5564, IEEE, apr 2015.

[10] J. van de Beek, M. Sandell, and P. Borjesson, "ML estimation of time and frequency offset in OFDM systems," *IEEE Transactions on Signal Processing*, vol. 45, pp. 1800–1805, jul 1997.

[11] Young-Hwan You, JoonBeom Kim, and Hyoung-Kyu Song, "Pilot-Assisted Fine Frequency Synchronization for OFDM-Based DVB Receivers," *IEEE Transactions on Broadcasting*, vol. 55, pp. 674–678, sep 2009.

[12] S. Coleri, M. Ergen, A. Puri, and A. Bahai, "Channel estimation techniques based on pilot arrangement in OFDM systems," *IEEE Transactions on Broadcasting*, vol. 48, pp. 223–229, sep 2002.

[13] R. Cardinali, F. Colone, C. Ferretti, and P. Lombardo, "Comparison of Clutter and Multipath Cancellation Techniques for Passive Radar," in *2007 IEEE Radar Conference*, pp. 469–474, IEEE, apr 2007.

[14] F. Colone, D. W. O'Hagan, P. Lombardo, and C. J. Baker, "A Multistage Processing Algorithm for Disturbance Removal and Target Detection in Passive Bistatic Radar," *IEEE Transactions on Aerospace and Electronic Systems*, vol. 45, pp. 698–722, apr 2009.

[15] C. Schwark and D. Cristallini, "Advanced multipath clutter cancellation in OFDM-based passive radar systems," in *2016 IEEE Radar Conference (RadarConf)*, pp. 1–4, IEEE, may 2016.

[16] G. Chabriel, J. Barrere, G. Gassier, and F. Briolle, "Passive Covert Radars using CP-OFDM signals. A new efficient method to extract targets echoes," in *2014 International Radar Conference*, pp. 1–6, IEEE, oct 2014.